Limitation of energy deposition in classical *N* body dynamics

D. Cussol
LPC Caen (IN2P3-CNRS/ISMRA et Université), 14050 Caen Cedex, France
(Received 4 September 2002; published 16 July 2003)

Energy transfers in collisions between classical clusters are studied with classical *N* body dynamics calculations for different entrance channels. It is shown that the energy per particle transferred to thermalized classical clusters does not exceed the energy of the least bound particle in the cluster in its ''ground state.'' This limitation is observed during the whole time of the collision, except for the heaviest system.

DOI: 10.1103/PhysRevC.68.014602 PACS number(s): 24.10.Cn, 25.70.−z

I. INTRODUCTION

The question of energy deposition in nuclei during nucleus-nucleus collisions is of great importance for nuclear matter studies. The maximum amount of energy that can be stored in hot equilibrated nuclei has been studied both experimentally [1–6] and theoretically [7,8]. Such studies have mainly been motivated by the determination of a plateau in the so called caloric curve (the evolution of the temperature with the excitation energy), which could be a signature of a first order liquid-gas phase transition [9,10].

Experimentally, a lot of work has been done to determine the amount of thermal energy stored in nuclei. For central collisions, large energy deposits up to 22.5*A* MeV have been determined [9,11]. Other studies have shown that the excitation energy in primary products in multifragmenting systems is around 3*A*-4*A* MeV [3,4,12,13], far below the total available energy in the center of mass frame. This energy does not seem to evolve strongly with the incident energy. These two measurements seem to be in contradiction. Possible limitations of energy deposition could result from prompt emission of energetic light charged particles at early times in the reaction [14–16].

Theoretically, the maximum energy that an equilibrated nucleus can withstand corresponds to the energy (or temperature) at which the surface tension vanishes. This is often characterized by a critical temperature T_c whose value is around 16 MeV [7,8]. This temperature is linked to the equation of state of nuclear matter. The main drawback of such studies is that they assume that the system is fully equilibrated and hence do not take into account possible limitations coming from the reaction mechanism.

The aim of the present paper is to study energy deposition during collisions between finite size systems in a well controlled framework. Results from the classical *N* body dynamics code [17] will be shown and the mechanism of energy deposition in classical clusters will be studied. We will consider in this paper the energy transferred to thermally equilibrated clusters, which corresponds to the energy that long-lived clusters can withstand. The paper is organized as follows. In the second section, the classical *N* body dynamics will be briefly described. The excitation energy in clusters will be shown for various systems and incident energies in the third section. The fourth section will be devoted to the mechanism of energy deposition in clusters. Conclusions will be drawn in the last section.

II. DESCRIPTION OF THE CODE

Let us start by describing the classical *N*-body dynamics code used in this paper. The basic ingredients of such a code are very simple. The dynamical evolution of each particle of the system is driven by the classical Newtonian equations of motion. The two-body potential used in the present work is a third degree polynomial whose derivatives are null at the range r_1 and at the distance of maximum depth r_{min}. The depth value is V_{min} and the value at $r=0$ is finite and equal to V_0. This potential has the basic properties of the Lennard-Jones potential used in other works [18,19]: a finite range attractive part and a repulsive short range part. To follow the dynamical evolution of the system an adaptative stepsize fourth-order Runge-Kutta algorithm is used [20]. The main difference with other works is that the time step Δt can vary: if the potential varies strongly, Δt is small and when the potential varies gently, Δt becomes larger. This allows a very high accuracy with shorter CPU time than for fixed time step algorithms. It requires an additional simulation parameter ϵ, which is adjusted to ensure the verification of conservation laws (energy, momentum, angular momentum) with a reasonable simulation time. The energy difference between the beginning and the ending simulation time is lower than 0.001%. This simulation has five free parameters: four linked to the physics (the interaction) and one linked to the numerical algorithm.

Since one wants to study the simplest case, neither long range repulsive interaction nor quantum corrections such as a Pauli potential have been introduced [21]. Additionally, no statistical decay code is applied to the excited fragments formed during the collision. The final products have to be regarded as ''primary'' products which would decay afterwards. Although most of the ingredients necessary for a correct description of atomic nuclei are missing from this simulation, it should be noted that the reaction mechanisms observed in nucleus-nucleus collisions are seen, and the properties of the ''ground states'' of such clusters are qualitatively close to those of nuclei [17].

In order to avoid any confusion with nuclear physics, the units used here are arbitrary and called simulation units (S.U.). The distance will then be in distance simulation units (D.S.U.), the energies in energy simulation units (E.S.U.), the reaction time in time simulation units (T.S.U.), and the velocities in velocity simulation units (D.S.U./T.S.U.).

TABLE I. Summary of systems.

$N_{projectile}$	N_{targ}	$E_{\mathrm{c.m.}}/N$ (E.S.U.)	E_{bind}/N fused (E.S.U.)	$E_{Least\text{-}Bound}$ fused (E.S.U.)	E^*/N fused (E.S.U.)	Number of events
13	13	25	−73.30	−50.86	35.17	1000
		45			55.17	1000
		65			75.17	1000
		85			85.17	1000
18	50	30	−93.60	−54.64	41.55	1000
		60			71.55	1000
		90			101.55	1000
		120			131.55	1000
34	34	30	−93.60	−54.64	42.04	1000
		60			72.04	1000
		90			102.04	1000
		120			132.04	1000
50	50	30	−98.93	−62.46	41.50	1000
		60			71.50	1000
		90			101.50	1000
		120			131.50	1000
100	100	30	−107.97(*)	−65.00(*)	39.03 (*)	100
		60			69.03(*)	100
		90			99.03(*)	100
		120			129.03(*)	100

For this study, 16 400 events have been generated. For a fixed projectile size N_{proj}, a fixed target size N_{targ}, and a fixed available energy in the center of mass $E_{\mathrm{c.m.}}/N$, the impact parameter b is randomly chosen assuming a flat distribution between 0 and $b_{max}=r(N_{proj})+r(N_{target})+r_1$, where $r(N_{proj})$ is the mean square radius of the projectile, $r(N_{target})$ is the mean square radius of the target, and r_1 the range of the potential. In the analyses, each event is weighted by its impact parameter value ($weight \propto b$). The systems and the energies studied here are summarized in Table I. As can be seen in Table I, the available energies in the center of mass frame $E_{\mathrm{c.m.}}/N$ have been chosen in such a way that the excitation energy of the fused cluster E^*/N is close to the binding energy of the fused cluster ($E_{\mathrm{c.m.}}/N=90$ E.S.U.), close to the energy of the least bound particle in the fused cluster ($E_{\mathrm{c.m.}}/N=60$ E.S.U.), far below ($E_{\mathrm{c.m.}}/N=30$ E.S.U.) or far above ($E_{\mathrm{c.m.}}/N=120$ E.S.U.) the binding energy of the fused cluster. The asterisks for the 100 + 100 system mean that these energies were estimated from the liquid-drop parametrization of the binding energies of the clusters [17]. In that case, the energy of the least bound particle is taken equal to −65 E.S.U. For each system, the excitation energy E^*_{fused} of the fused cluster is determined by

$$E^*_{fused}=E_{\mathrm{c.m.}}+E_{bind}(N_{proj})+E_{bind}(N_{targ})-E_{bind}(N_{fused}), \quad (1)$$

where $E_{bind}(N)$ is the binding energy of the cluster of size N.

In this unit system, the parameters of the reaction are the following: $V_0=540$ E.S.U., $V_{min}=-20$ E.S.U., $r_{min}=10$ D.S.U., and $r_1=15$ D.S.U. Typical mean square radii are around 10 D.S.U. for $N\approx 20$ and around 15 D.S.U. for $N \approx 70$ (for more information, see Ref. [17]). The time for a particle to go through a cluster ranges from 7 to 10 T.S.U. at the lowest available energies ($E_{\mathrm{c.m.}}/N \leqslant 30$ E.S.U.) and ranges from 3 to 5 T.S.U. at the highest available energies ($E_{\mathrm{c.m.}}/N \geqslant 90$ E.S.U.). As seen in Ref. [17], fusionlike mechanisms and particle transfer mechanisms are observed at low $E_{\mathrm{c.m.}}/N$ values ($E_{\mathrm{c.m.}}/N \lesssim 60$ E.S.U.), while multifragment production and neck formation and breakup are dominant at high $E_{\mathrm{c.m.}}/N$ values ($E_{\mathrm{c.m.}}/N$ 60 E.S.U.). As will be seen in Sec. III, typical thermalization times for such systems ranges from 15 to 20 T.S.U.

III. ENERGY DEPOSITION IN FINAL CLUSTERS

In this section, we will be interested in the energy deposition in clusters at the simulation time $t=200$ T.S.U. At this stage, the clusters are well separated from each other in configuration space. As will be seen later, these clusters are thermally equilibrated. They can be viewed as primary clusters. For this first simple analysis, the clusters have been identified by using the minimum spanning tree method (labeled MST), which assumes that two particles belong to the same cluster if they are in potential interaction, i.e., if their relative distance is below the range r_1 of the potential.

A. Variations of the energy deposition with the velocity of the cluster

In Figs. 1–5 are plotted the evolution of the excitation energy E^*/N of the cluster and its parallel velocity $V_{\parallel}$ for the whole impact parameter range and for different available energies in the center of mass. The excitation energy of each

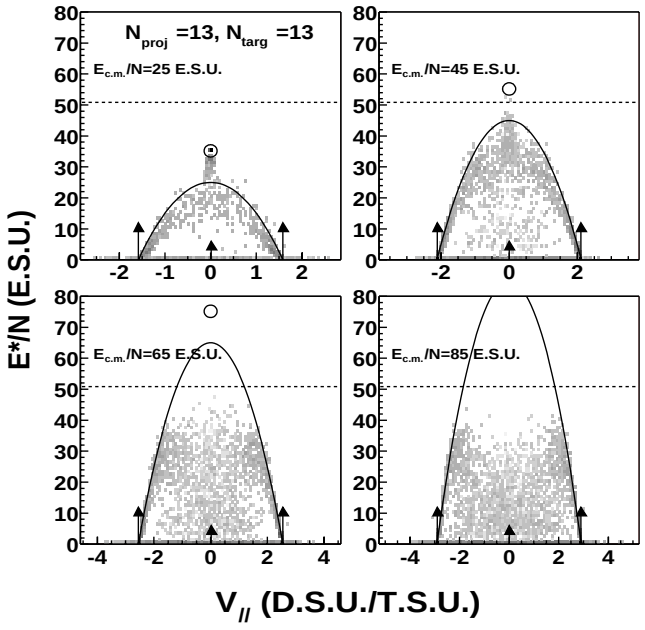

FIG. 1. Excitation energy of clusters versus their parallel velocity for $N_{proj}=13$ on $N_{targ}=13$ collisions at different available energies in the center of mass. On each panel, the full line corresponds to the expected evolution for a pure binary process, the dashed horizontal line corresponds to the energy of the least bound particle for $N=26$, and the circle corresponds to the expected values for the fused system. On each plot, the darkest gray regions correspond to the highest differential cross section values.

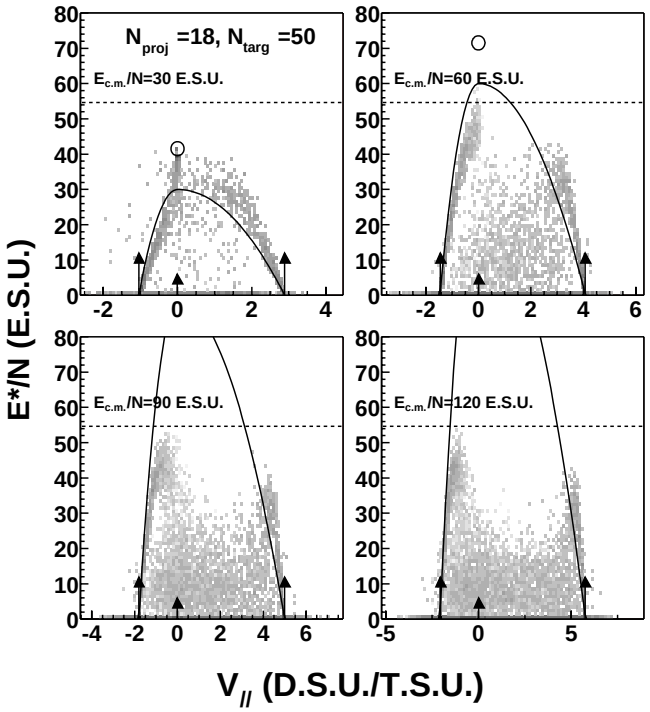

FIG. 3. Same as Fig. 1, but for $N_{proj}=18$ on $N_{targ}=50$ collisions. On each panel the dashed horizontal line corresponds to the energy of the least bound particle for $N=68$.

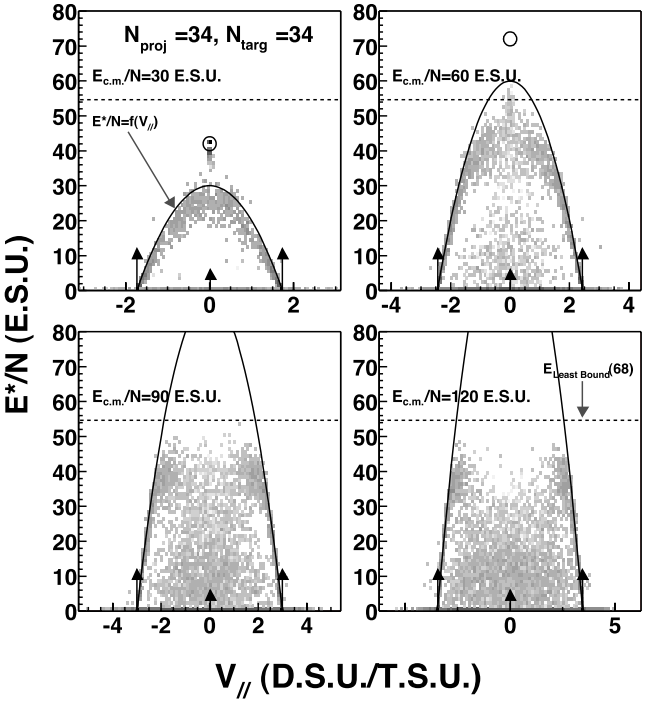

FIG. 2. Same as Fig. 1, but for $N_{proj}=34$ on $N_{targ}=34$ collisions On each panel the dashed horizontal line corresponds to the energy of the least bound particle for $N=68$.

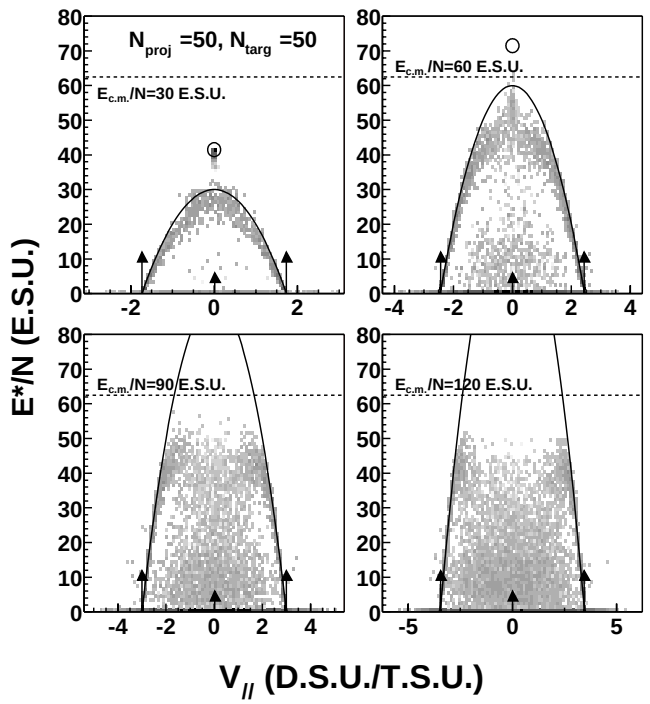

FIG. 4. Same as Fig. 1, but for $N_{proj}=50$ on $N_{targ}=50$ collisions. On each panel the dashed horizontal line corresponds to the energy of the least bound particle for $N=100$.

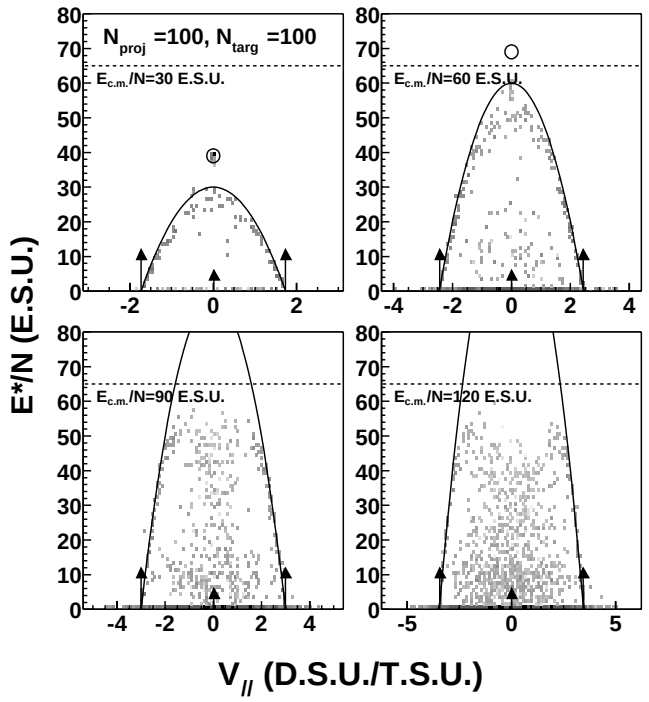

FIG. 5. Same as Fig. 1, but for $N_{proj}=100$ on $N_{targ}=100$ collisions. On each panel the dashed horizontal line corresponds to the estimated energy of the least bound particle for $N=200$.

cluster is simply the difference between the total energy (potential plus kinetic) and the ''ground state'' energy of the cluster:

$$E^*=\sum_i E_i^{kin}+\sum_{i,j,i>j} V(|\vec{r}_i-\vec{r}_j|)-E_{bind}(N), \qquad (2)$$

where E_i^{kin} is the kinetic energy of the particle i in the cluster's center of mass, $V(|\vec{r}_i-\vec{r}_j|)$ the potential energy between the particles i and j, $E_{bind}(N)$ the binding energy of the cluster, and N its number of particles. This excitation energy is determined at the end of the calculation corresponding to $t=200$ T.S.U. As will be seen in the following section, this energy is very close to the one obtained at the separation time of the clusters (the smallest time at which clusters can be identified), since in this time range the emission of monomers or small clusters by the primary clusters (evaporation) is very weak and the clusters have no time to cool down significantly [18]. On each panel of the figures, the full line corresponds to the expected correlation between E^*/N and $V_{\parallel}$ for a pure binary scenario, i.e., the excitation energy is only due to the velocity damping of each partner, without any particle exchange between them. This excitation energy is then determined by

$$E^*=\frac{1}{2}\frac{m_p m_t}{m_p+m_t}(v_{rel,max}^2-v_{rel}^2), \qquad (3)$$

where m_p and m_t are the projectile and the target mass, respectively, $v_{rel,max}$ the initial relative velocity between the projectile and the target, and v_{rel} is the relative velocity between the projectile and the target after interaction. The mass of each cluster is proportional to the number of particles $m(N)=m_{particle}\times N$ where $m_{particle}=20$ S.U. The initial relative velocity is given by

$$v_{rel,max}=\sqrt{2E_{c.m.}\frac{m_p+m_t}{m_p m_t}}. \qquad (4)$$

The small circle displayed on each panel is centered around the expected values of velocity and excitation energy for the fused system. The horizontal dashed line corresponds to the energy of the least bound particle $E_{Least\text{-}Bound}$ for the fused system $N=N_{proj}+N_{target}$. This energy is determined for the stable clusters (''ground state'') and is defined as follows:

$$E_{Least\text{-}Bound}=\max_{j=1,N}\left[\sum_{i\neq j} V(r_{ij})\right], \qquad (5)$$

where r_{ij} is the relative distance between the particles i and j and $V(r_{ij})$ is the value of the two-body potential. As has been shown in Ref. [17], this energy varies dramatically with N. In their ''ground states'' the clusters are small crystals and the $E_{Least\text{-}Bound}$ value is mainly due to geometrical effects (number of neighbors of a particle at the surface). Such variations are well known in cluster physics [22].

At low $E_{\mathrm{c.m.}}/N$ values ($E_{\mathrm{c.m.}}/N=25$ E.S.U. for the 13+13 system and $E_{\mathrm{c.m.}}/N=30$ E.S.U. for the others), the points are slightly below the full line. This means that the excitation energy is strongly linked to the velocity damping. In that case, the collisions lead to the formation of excited projectilelike and targetlike clusters. The small shift is due to mass transfers between the projectile and the target, and to promptly emitted clusters. The area corresponding to the fused system is well populated, showing that a complete fusion process occurs. At intermediate energies ($E_{\mathrm{c.m.}}/N=45$ E.S.U. for the 13+13 system and $E_{\mathrm{c.m.}}/N=60$ E.S.U. for the others), the distribution of points is roughly compatible with the pure binary process hypothesis (formation of excited projectilelike and targetlike clusters) except for cluster velocities that lead to excitation energies per particle higher than $E_{Least\text{-}Bound}(N_{fused})$ (where $N_{fused}=N_{proj}+N_{target}$) in the pure binary process picture. For these clusters, E^*/N is always smaller than $E_{Least\text{-}Bound}(N_{fused})$. The complete fusion process area, located above $E_{Least\text{-}Bound}(N_{fused})$, is empty. In that case, as will be seen in the following section, incomplete fusion process occurs. For the two highest energies, this trend is enhanced. Around the projectile and the target velocity the projectilelike and targetlike clusters have an excitation energy compatible with the pure binary process hypothesis. Around the center of mass velocity, when this picture would give excitation energies per particle higher than $E_{Least\text{-}Bound}(N_{fused})$, one finds clusters at small excitation energies. The energy of the least bound particle seems to be a limit to the excitation energy which can be stored in these classical clusters.

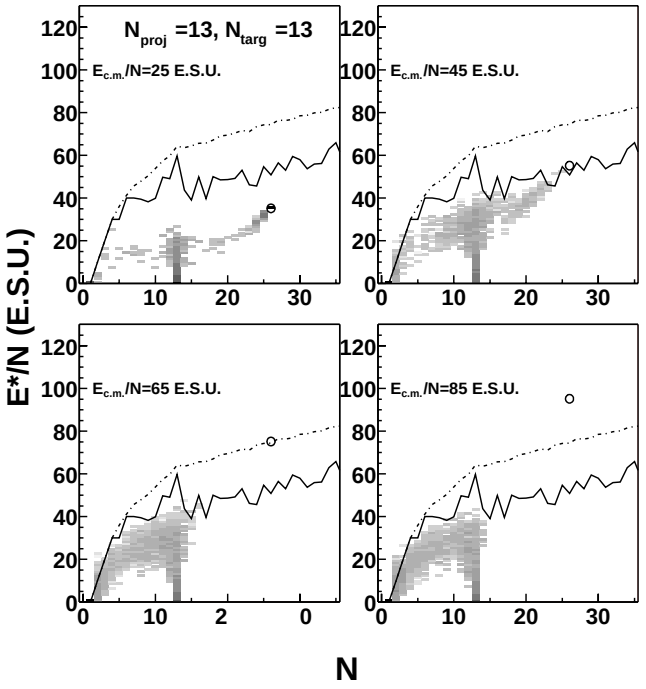

FIG. 6. Excitation energy of clusters versus N for $N_{proj}=13$ on $N_{targ}=13$ collisions at different available energies in the center of mass. On each panel, the full line corresponds to the energy of the least bound particle, the dash-dotted line corresponds to the binding energy per particle, and the circle corresponds to the expected values for the fused system. On each plot, the darkest gray regions correspond to the highest differential cross section values.

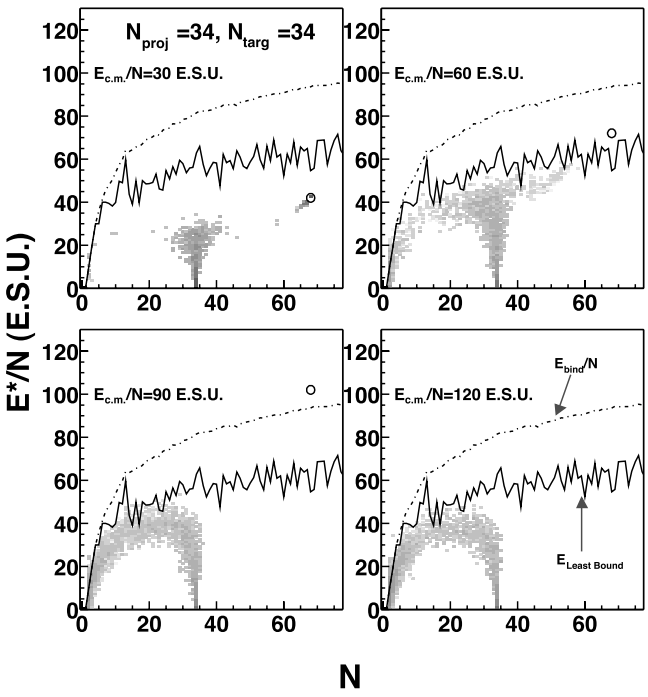

FIG. 7. Same as Fig. 6, but for $N_{proj}=34$ on $N_{targ}=34$ collisions.

B. Variations of the energy deposition with the size of the cluster

This limitation can be more clearly seen when the excitation energy E^*/N is plotted as a function of N, as in Figs. 6–10. On each panel, the full line corresponds to the energy of the least bound particle, $E_{Least\text{-}Bound}$, in the cluster and the dashed line to the binding energy per particle, E_{bind}/N. As in Figs. 1–5, the small circle corresponds to the expected values for the fused system. At low energy, the area corresponding to complete fusion is filled and all the available energy can be stored as excitation energy. But for higher energies, one can clearly see that for each fragment size, E^*/N never overcomes $E_{Least\text{-}Bound}$. At intermediate energy, clusters with sizes higher than the projectile size and the target size can be seen. This area corresponds to an incomplete fusion process. For the two highest energies, the plots are almost identical: there is no more fusion (the small circle area is empty) and the clusters are smaller than the target and the projectile. One can notice that E^*/N never reaches the binding energy E_{bind}/N except for small clusters where E_{bind}/N and $E_{Least\text{-}Bound}$ are equal. The energy of the least bound particle in the cluster $E_{Least\text{-}Bound}$ is an upper limit for the energy per particle which can be stored in the cluster, whatever the system size, the available energy in the center of mass, and the asymmetry of the entrance channel.

C. Variations of the energy deposition with the impact parameter and the available energy in the center of mass

Figure 11 shows the variations of the average excitation energy per particle $\langle E^*/N\rangle$ with the reduced impact param-

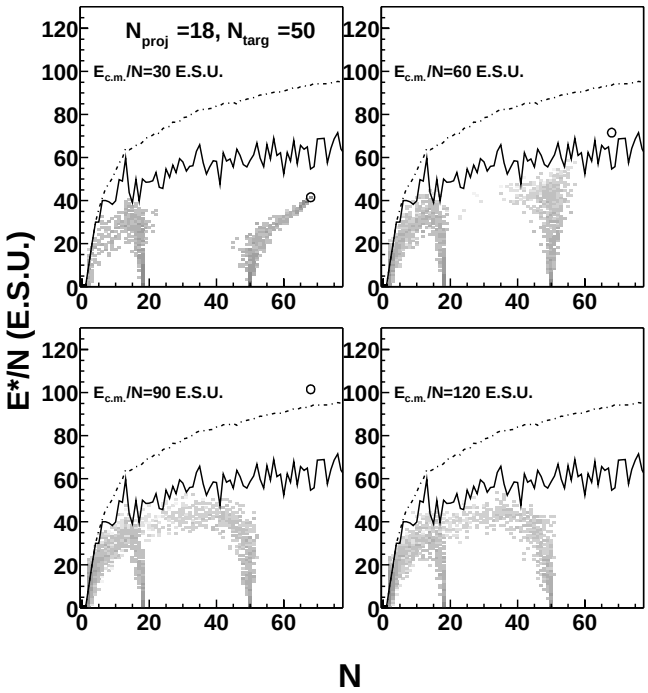

FIG. 8. Same as Fig. 6, but for $N_{proj}=18$ on $N_{targ}=50$ collisions.

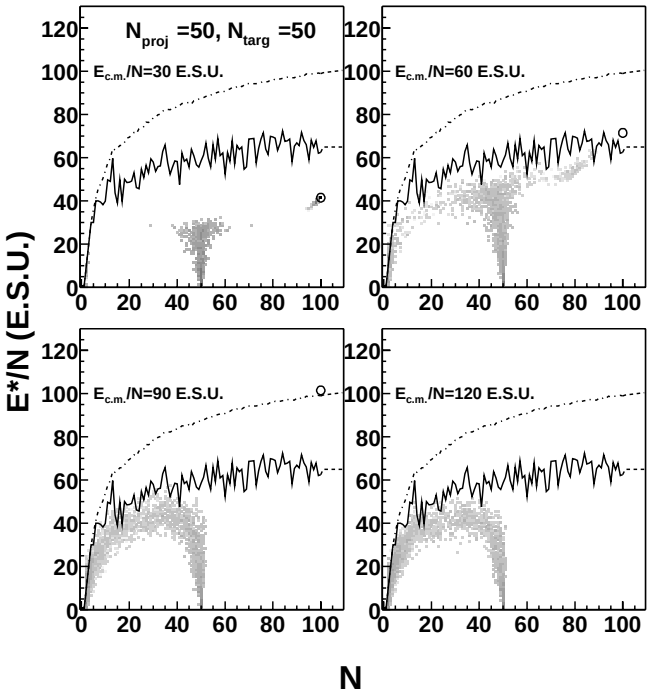

FIG. 9. Same as Fig. 6, but for $N_{proj}=50$ on $N_{targ}=50$ collisions.

eter $b_{red}=b/b_{max}$ for different available energies in the center of mass frame $E_{\mathrm{c.m.}}/N$. The average is calculated for clusters with N greater than or equal to 3. Each panel corresponds to a system. The squares correspond to the lowest $E_{\mathrm{c.m.}}/N$ values, the triangles to $E_{\mathrm{c.m.}}/N$ values close to $E_{Least\text{-}Bound}$, the diamond to $E_{\mathrm{c.m.}}/N$ values close to E_{bind}/N, and the circles to the highest $E_{\mathrm{c.m.}}/N$ values. As in the previous figures, the average excitation energy is limited around 40 E.S.U. except for the 100+100 system for which the maximum energy reached is 50 E.S.U. at $E_{\mathrm{c.m.}}/N=60$ E.S.U.

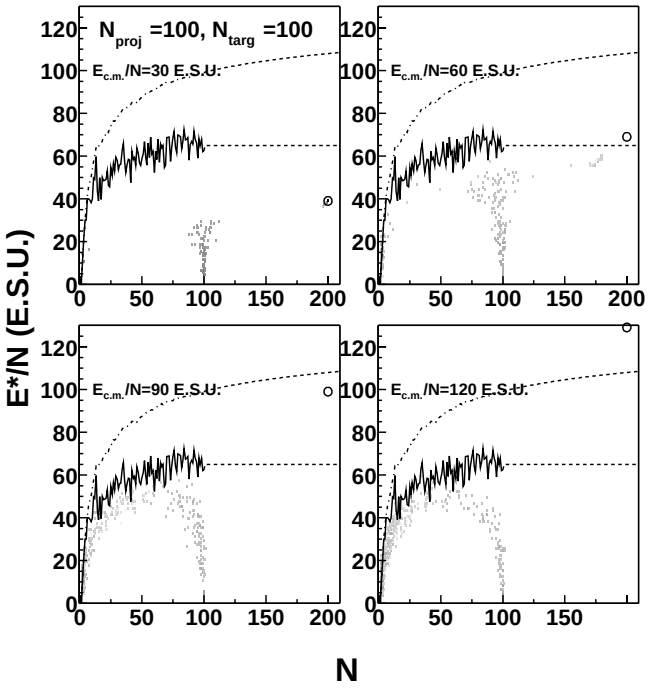

FIG. 10. Same as Fig. 6, but for $N_{proj}=100$ on $N_{targ}=100$ collisions. The dashed lines on each panel correspond to the extrapolated values of the binding energy (upper line) and the extrapolated energy of the least bound particle (lower line) for $N>100$.

At the lowest energy, for symmetric systems, $\langle E^*/N\rangle$ increases when b_{red} decreases down to $b_{red}=0.4$, and then is constant at $\langle E^*/N\rangle\approx 40$ E.S.U. below. This saturation is due to the occurrence of fusion: the maximum excitation energy is reached by the fused system. For the asymmetric system 18+50, saturation occurs at smaller impact parameters. For intermediate energies, the picture is roughly the same. But although the available energy is higher, the maximum $\langle E^*/N\rangle$ value is almost the same as for the lowest available energy. In that case, an incomplete fusion process occurs and the excitation energy of the heaviest cluster is limited by the energy of its least bound particle, which is well below the expected excitation energy of the fused system. For the two highest energies, $\langle E^*/N\rangle$ increases when b_{red} decreases down to $b_{red}=0.4$ and then $\langle E^*/N\rangle$ decreases when b_{red} decreases. This effect results from the lower cluster sizes for the most central collisions, which at these energies produce several clusters of intermediate sizes. Indeed, the smaller the cluster size is, the lower the upper limit in energy storage. Since clusters have a smaller size for central collisions, the $\langle E^*/N\rangle$ decreases consequently. This evolution does not seem to depend strongly on the total system size or on the entrance channel asymmetry.

The same evolution is seen in Fig. 12, which shows the evolution of the ratio $\langle E^*/N\rangle/(E^*/N)_{max}$, where $(E^*/N)_{max}$ corresponds to the maximum excitation energy expected for the fused systems. For low energies, this ratio continuously increases when b_{red} decreases and is close to 1 below $b_{red}\approx 0.4$: this corresponds to the occurrence of the fusion process. This value of 1 is reached for b_{red} below 0.2 for the 18+50 system. This difference can be understood quite easily: for a fixed $E_{\mathrm{c.m.}}/N$ value, the relative velocity between the projectile and the target is higher for an asymmetric system than for a symmetric one [see Eq. (4)]. This leads to an interaction time smaller for the asymmetric system than for a symmetric one and then to less efficient energy deposition in the clusters. For higher energies, this value of 1 is never reached. The maximum value even decreases when $E_{\mathrm{c.m.}}/N$ increases: the relative amount of energy stored in clusters decreases when the available energy increases.

D. Discussion

These studies show that in classical systems, the energy storage in clusters is limited. Such a saturation was observed for two-dimensional classical systems [23]. This limitation is only linked to the intrinsic properties of the cluster: the energy deposition cannot be higher than the energy of the least bound particle in the cluster.

This limitation of excitation energy can be understood quite easily. The least bound particle remains bound to the

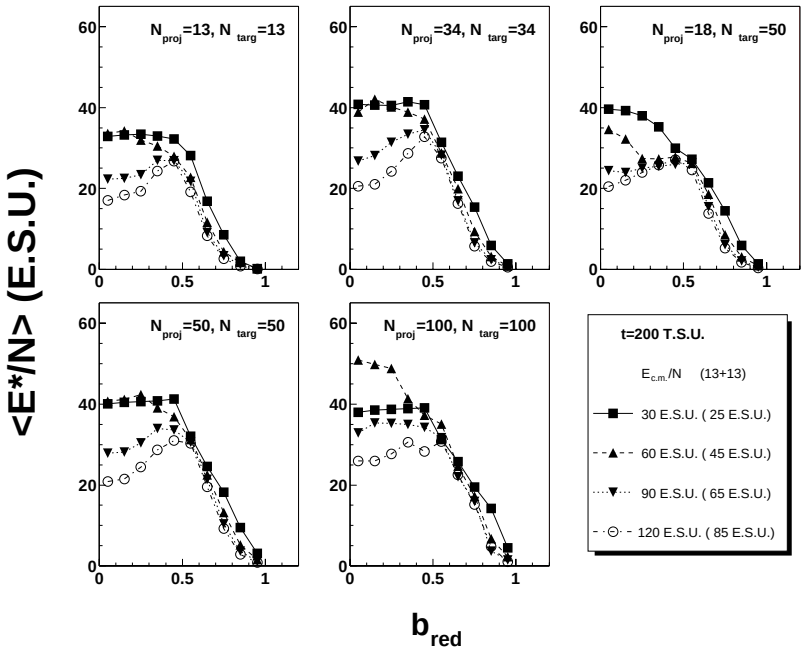

FIG. 11. Average excitation energy stored in the clusters as a function of the reduced impact parameter. The different lines and symbols correspond to different values of the available energy per particle in the center of mass frame. The $E_{\mathrm{c.m.}}/N$ values indicated in parentheses correspond to the 13+13 system. See text for details.

cluster only if its total energy is negative, i.e., its kinetic energy due to the excitation is below its potential one. If one assumes that the excitation energy is roughly equally shared over all particles in the cluster, when the kinetic energy balances the potential energy of the least bound particle, this particle is no longer bound to the cluster and quickly escapes. To be observed for a long time (greater than the thermalization time), the excited cluster must have an excitation energy per particle below the energy of the least bound particle.

The mechanism of energy deposition in classical N body clusters seems to be the following one: the excitation is mainly driven by the velocity damping of the two partners and to a lesser extent by exchanges of particles between them. Once the energy of the least bound particle is reached, unbound particles and/or clusters escape quickly and keep an excitation energy per particle below the energy of the least bound one. As a consequence, the highest energy deposition per particle can only be obtained at $E_{\mathrm{c.m.}}/N$ energies close to $E_{Least\text{-}Bound}$. For higher available energies, the system fragments quickly, leaving rather ''cold'' clusters around the center of mass velocity. The energy in excess is stored in the kinetic energies of the clusters. A similar mechanism could be an explanation of the apparent saturation of primary fragments' excitation energies observed for central collisions of the Xe+Sn system when the incident energy increases from 32A to 50A MeV [13,12]. This could also be an explanation for the limitation of temperature values around 5 MeV by

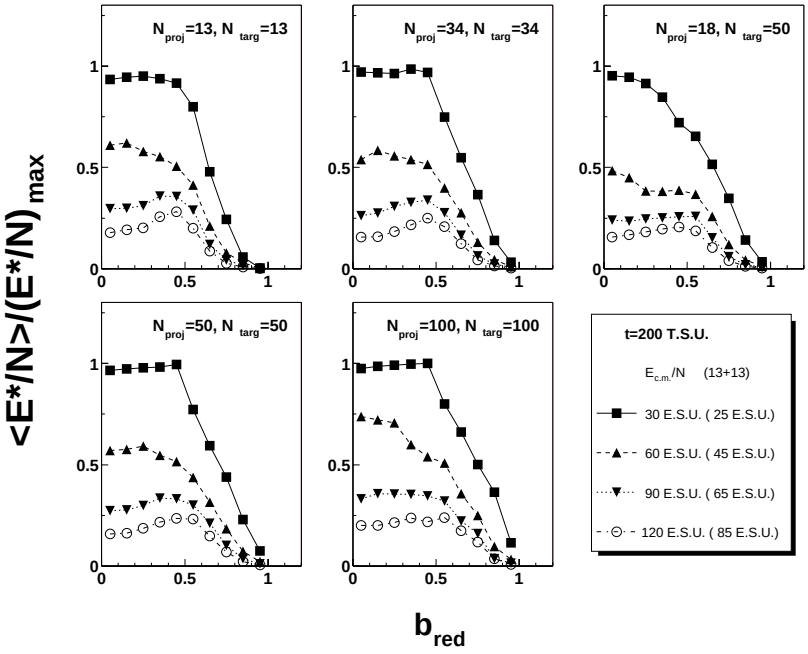

FIG. 12. Average amount of available energy stored in the clusters as a function of the reduced impact parameter. The different lines and symbols correspond to different values of the available energy per particle in the center of mass frame. The $E_{\mathrm{c.m.}}/N$ values indicated in parentheses correspond to the 13+13 system. See text for details.

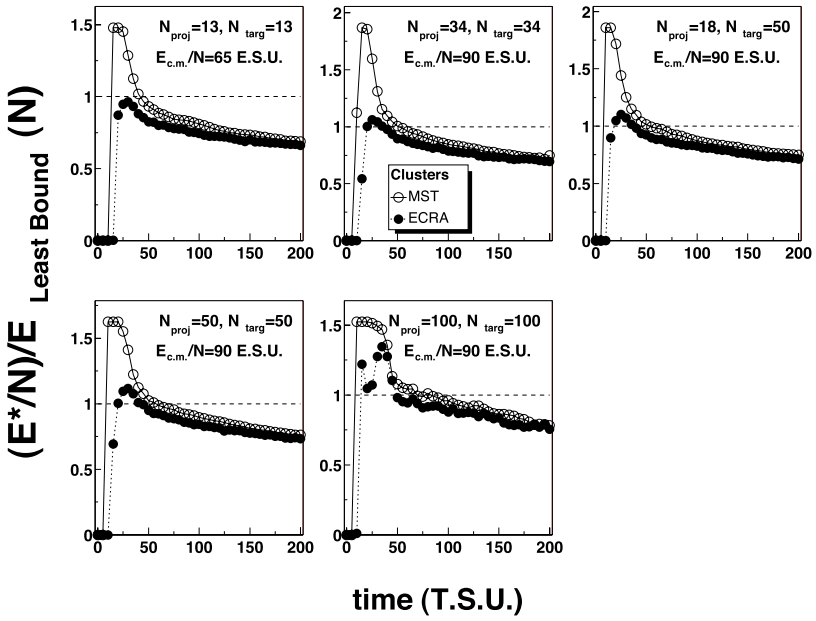

FIG. 13. Variation of the ratio $(E^*/N)/E_{Least\text{-}Bound}$ with time for various systems and for central collisions ($b_{red}<0.1$) when the available energy in the center of mass is close to the binding energy of the fused system. The open circles correspond to the MST clusters and the full circles to the ECRA clusters.

using isotope ratio methods or population ratio methods [9,10]. Such a limitation has been observed in the fragmentation of uranium projectiles at relativistic energies [4]. This limitation was also suggested by the observation of the saturation of the evaporated neutron multiplicity when the incident energy increases [5].

Provided that this conclusion can be applied in nuclear physics, i.e., if quantum effects and Coulomb interaction do not modify strongly the above picture, the maximum energy per nucleon which can be stored in thermalized hot nuclear fragments would never exceed the energy of the least bound nucleon. This energy would correspond to the energy of the last populated level. If this assertion is true, it would be in contradiction with several experimental works in which high energy depositions (up to 20*A* MeV) were measured [11,9,3]. This discrepancy may result from the calorimetry analyses used in these papers, whereas E^*/N is directly extracted in this work.

One has to be careful because the observations made here are for a fixed simulation time. At the early stages of the collision, higher energy deposition could be reached for short times. The following section will be devoted to the evolution of this energy deposition with the reaction time.

IV. EVOLUTION OF THE ENERGY DEPOSITION WITH TIME

The aim of the present section is to check to which extent the limitation of the energy deposition observed for final (long simulation times) thermally equilibrated clusters is true during the collision. Since the limitation is linked to the energy of the least bound particle in the cluster, we will follow the ratio of the excitation energy per particle to the energy of the least bound particle $(E^*/N)/E_{Least\text{-}Bound}(N)$ with collision time.

Such an evolution is shown in Fig. 13 for MST clusters for central collisions ($b_{red}<0.1$) for all systems at $E_{\mathrm{c.m.}}/N=90$ E.S.U. (65 E.S.U. for the 13+13 system). It is seen that for MST clusters (open circles) very high energies can be found, up to the maximum excitation energy. This means that very excited systems could be formed at the early stages of the collision. But one has to check first if this transferred energy is equally shared between all degrees of freedom and hence if these intermediate clusters are thermalized.

One way to check this thermalization is to follow the ratio between the dispersion of the distribution of the kinetic energy of particles $\sigma(E_{kin})$ in the cluster and its average value $\langle E_{kin}\rangle$. For a thermalized system, the value of this ratio is well defined: it is equal to $\sqrt{2/3}$ in the canonical ensemble, and equal to $\sqrt{(2N-2)/(3N-1)}$ in the microcanonical ensemble [24], where N is the number of particles in the cluster. The time evolution of $R_{thermalization}=[\sigma(E_{kin})/\langle E_{kin}\rangle]/\sqrt{(2N-2)/(3N-1)}$ is displayed in Fig. 14 for the 34+34 system (first row) and the 50+50 system (second row) at the two highest $E_{\mathrm{c.m.}}/N$ values (90 E.S.U., left column, and 120 E.S.U., right column). A value close to 1 indicates that the cluster is thermalized. Let us first follow the evolution of the ratio for MST clusters (open circles). The thermalization of clusters is reached at $t\approx 50$ T.S.U. for both systems at $E_{\mathrm{c.m.}}/N=90$ E.S.U. The excitation energy per particle of the MST clusters at this time (see Fig. 13, open circles) is close to or below the energy $E_{Least\text{-}Bound}$ of the least bound particle in the cluster. For later times, the ratio slightly varies around 1, showing that clusters stay thermalized even if evaporation of light clusters occurs. The same conclusion can be drawn at $E_{\mathrm{c.m.}}/N=120$ E.S.U. for which the thermalization is reached at $t\approx 35$ T.S.U. when the excitation energy per particle is very close to $E_{Least\text{-}Bound}$. From this simple study, one can conclude that the highly excited intermediate cluster is not thermalized, and that thermalized clusters have an excitation energy per particle close to or below $E_{Least\text{-}Bound}$.

It has been found in earlier works that such systems are indeed composed of several small clusters at early times [25,26,19]. The size distributions of these clusters have been

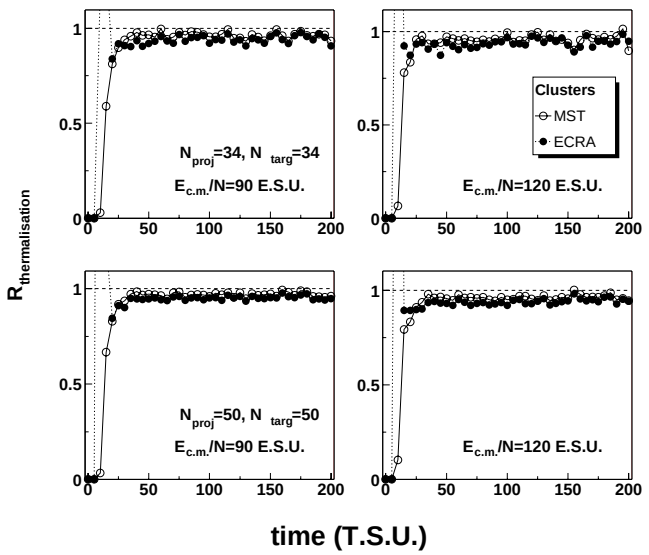

FIG. 14. Variation of the ratio $[(\sigma(E_{kin})/\langle E_{kin}\rangle]/\sqrt{2N/(3N-2)}$ with time for the 34+34 system (first raw) and the 50+50 system (second raw), for central collisions ($b_{red}<0.1$) at the two highest $E_{\mathrm{c.m.}}/N$ values (90 E.S.U., left column, and 120 E.S.U., right column). The open circles correspond to the MST clusters and the full circles to the ECRA clusters.

found to be almost identical to those identified after their separation [19]. The problem is how to identify these clusters. In that respect, the MST algorithm is no longer suited since particles close to each other at these early stages are not necessarily bound at later times. Different methods have been developed to identify clusters. One is to assume that two particles belong to the same cluster if they are bound, i.e., if their relative energy is negative. These clusters have been labeled Coniglio-Klein clusters (CK clusters) or MSTE clusters in other works. Another way to define clusters is to find at each time step the most bound partition of particles in clusters. This algorithm is described in detail in Ref. [27] and is called early cluster recognition algorithm (ECRA). The latter will be used in the present work.

In Fig. 13 the evolution of $(E^*/N)/E_{Least\text{-}Bound}$ with the collision time is shown for ECRA (filled circles) clusters. Above $t\approx 50$ T.S.U. both algorithms (MST and ECRA) give the same results: clusters are well separated in the configuration space. At this time, clusters do not interact anymore with each other: this corresponds to the ''freeze-out'' configuration assumed in statistical multifragmentation models [28,29]. One has to notice that this time coincides with the thermalization time found in the previous paragraph. The thermalization of ECRA clusters (see Fig. 14, filled circles) is also reached at the ''freeze-out'' time. After this time, clusters have an excitation energy below $E_{Least\text{-}Bound}$ (ratio below 1). But for earlier times, the configuration is more complex. While MST clusters reach very high excitation energies per particle, the ratio for ECRA clusters is always around or below 1, except for the 100+100 system. Apart for the latter system, the limitation observed in the preceding section seems to be still true all along the collision time. But what leads to the difference observed for the 100+100 system?

Indeed, for such a heavy system, preformed clusters remain together long enough to interact strongly. If one of the particles escapes from one of these clusters, the probability that it is captured by another cluster is high. In that respect the clusters are acting as a confining wall and inhibiting quick escapes of the most energetic particles. These interactions between preformed clusters prevent their thermalization before the ''freeze-out'' time. It can be seen in Fig. 13 that the maximum value of the ratio is higher for heavier systems. This effect should be reduced when the time during which clusters interact is reduced, i.e., when the available energy increases. This is observed in Fig. 15, which shows the evolution of the ratio with time for $E_{\mathrm{c.m.}}/N=120$ E.S.U. ($E_{\mathrm{c.m.}}/N=85$ E.S.U. for the 13+13 system). At this energy, the reaction times are smaller and the ratio is always close to or below 1.

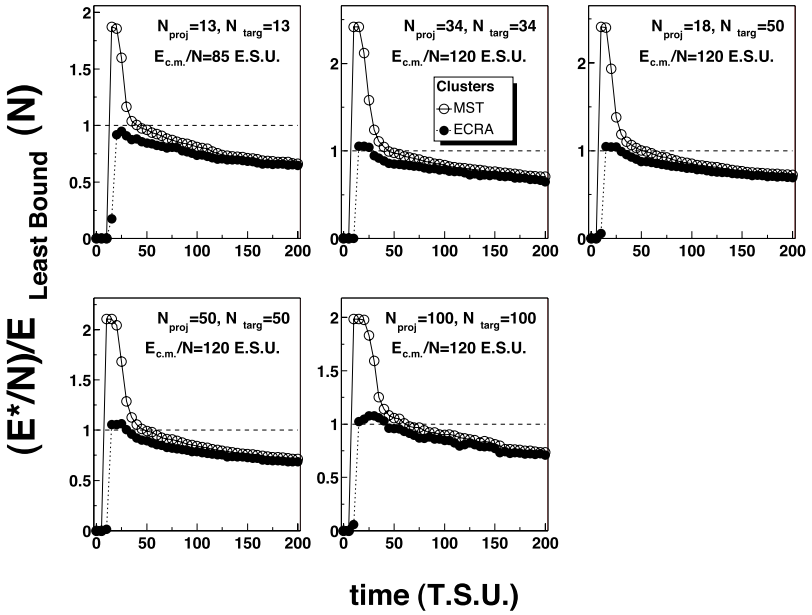

FIG. 15. Variation of the ratio $(E^*/N)/E_{Least\text{-}Bound}$ with time for various systems and for central collisions ($b_{red}<0.1$) when the available energy in the center of mass is close to the most bound particle in the fused system. The open circles correspond to the MST clusters and the full circles to the ECRA clusters.

It could be argued that the observed evolution of ECRA clusters is only due to the algorithm of cluster recognition used. Since one tries to find the most bound partition, this could minimize the energies of clusters. It is indeed observed that ECRA clusters have an excitation energy below that of the MST clusters. One can make two remarks. The first one is that the $E_{Least\text{-}Bound}$ has not been used to determine the ECRA clusters. There is hence no reason to find $E_{Least\text{-}Bound}$ as an upper limit for the excitation energy for ECRA clusters. The second remark is that ECRA clusters with energies higher than $E_{Least\text{-}Bound}$ can be found in some specific cases (see Fig. 13 for the 100+100 system) when particles cannot easily escape from clusters. The evolutions seen for ECRA clusters are then more likely due to the physics of the collision rather than to the definition of these clusters.

As in Sec. II, the energy that can be stored in a thermalized cluster seems to be limited almost throughout the collision time. The detailed analysis shows that the exact value of this limitation may depend on reaction time and on the system size. Before the ''freeze-out'' time, this limit can be higher than $E_{Least\text{-}Bound}$ if clusters are close enough together for a long time. This has been observed for the heaviest systems and for an $E_{\mathrm{c.m.}}/N$ value close to the binding energy of the fused system. After the ''freeze-out'' time, all clusters have an excitation energy per particle below $E_{Least\text{-}Bound}$.

If clusters are excited in a confining ''box'' (wall, neighboring clusters) which prevents quick emission of monomers and small clusters, very high excitation energies can be deposited in these clusters: they are artificially bound by the confining wall or the neighboring clusters. If clusters are ''free'' (no confining wall, no neighboring clusters), the energy deposition per particle cannot exceed $E_{Least\text{-}Bound}$.

V. CONCLUSIONS

The energy deposition in clusters in cluster-cluster collisions has been studied in the framework of classical N body dynamics. The mechanism of energy deposition seems to be the following: the excitation energy of clusters is mainly due to the relative velocity damping between the projectile and the target, and to a lesser extent to particle exchanges between them. The excitation per particle of thermalized clusters is limited by the energy of the least bound particle in the cluster. In the low energy regime ($E_{\mathrm{c.m.}}/N < E_{Least\text{-}Bound}$), the excitation energy increases when the impact parameter decreases and reaches its maximum value for the most central collisions ($b_{red} \leqslant 0.5$). For the intermediate energy regime ($E_{\mathrm{c.m.}}/N \approx E_{Least\text{-}Bound}$) the picture is almost the same, except that for central collisions the incomplete fusion system has an excitation energy per particle close to $E_{Least\text{-}Bound}$. For high energy regimes ($E_{\mathrm{c.m.}}/N \geqslant E_{Bind}/N$) the maximum energy deposition is found for intermediate impact parameters ($b_{red} \approx 0.5$), whereas for central collisions clusters are less excited and E^*/N is always lower than $E_{Least\text{-}Bound}$.

This limitation of energy deposition is almost verified throughout the collision. High energy deposits ($E^*/N \approx 1.4 E_{Least\text{-}Bound}$) have been found for ECRA clusters and for heavy systems before the ''freeze-out'' time, which coincides with the thermalization time of the clusters. This effect is mainly due to the time scales of the reaction. Above the ''freeze-out'' (thermalization) time, the excitation energy per particle of free clusters is below $E_{Least\text{-}Bound}$.

This limitation of energy deposition in thermalized clusters could be an explanation for rather low excitation energies found in primary fragments in nucleus-nucleus collisions. If this limitation is also true for nuclei, this would be in contradiction with many experimental works in which excitation energies well above the binding energy have been determined. This could shed new light on caloric curve analyses and on phase transition studies.

ACKNOWLEDGMENT

I would like to warmly thank J. D. Frankland for his careful reading of this paper and for valuable suggestions.

[1] D. Jiang, *et al.*, Nucl. Phys. **503**, 560 (1989).
[2] E. Vient, *et al.*, Nucl. Phys. **A571**, 588 (1994).
[3] J.B. Natowitz, R. Wada, T. Keutgen, A. Makeev, L. Qin, P. Smith, and C. Hamilton, Phys. Rev. C **65**, 034618 (2002).
[4] K. H. Schmidt, M. V. Ricciardi, A. Botvina, and T. Enqvist (unpublished).
[5] J. Galin and U. Jahnke, J. Phys. G **20**, 1105 (1994).
[6] J.C. Steckmeyer *et al.*, INDRA Collaboration, Nucl. Phys. **A686**, 537 (2001).
[7] S. Levit, P. Bonche, and D. Vautherin, Nucl. Phys. **A427**, 278 (1984).
[8] S. Levit, P. Bonche, and D. Vautherin, Nucl. Phys. **A436**, 265 (1986).
[9] Y.G. Ma *et al.*, INDRA Collaboration, Phys. Lett. B **390**, 41 (1998).
[10] J. Pochodzalla, *et al.*, Phys. Rev. Lett. **75**, 1040 (1995).
[11] B. Borderie *et al.*, INDRA Collaboration, Phys. Lett. B **388**, 224 (1996).
[12] S. Hudan *et al.*, INDRA Collaboration, in Proceedings of the XXXVIII International Winter Meeting on Nuclear Physics, 2002, edited by I. Iori and A. Moroni.
[13] N. Marie *et al.*, INDRA Collaboration, Phys. Rev. C **58**, 256 (1998).
[14] T. Lefort *et al.*, INDRA Collaboration, Nucl. Phys. **A662**, 397 (2000).
[15] D. Doré *et al.*, INDRA Collaboration, Phys. Lett. B **491**, 15 (2000).
[16] D. Doré *et al.*, INDRA Collaboration, Phys. Rev. C **63**, 034612 (2001).
[17] D. Cussol, Phys. Rev. C **65**, 054614 (2002).
[18] A. Strachan and C. Dorso, Phys. Rev. C **59**, 285 (1999).
[19] X. Campi, H. Krivine, and N. Sator, Nucl. Phys. **A681**, 458 (2000).
[20] W. H. Press, B. P. Flannery, S. A. Teukolsky, and W. T. Vetterling, *Numerical Recipes* (Cambridge University Press, Cambridge, England, 1989).

[21] C. Dorso, S. Duarte, and J. Randrup, Phys. Lett. B **188**, 287 (1987).
[22] D.J. Wales and J.P.K. Doye, J. Phys. Chem. A **101**, 5111 (1997).
[23] A. Strachan and C.O. Dorso, Phys. Rev. C **58**, R632 (1998).
[24] J.A. Lopez and J. Randrup, Nucl. Phys. **A503**, 183 (1989).
[25] R. Nebauer *et al.*, INDRA Collaboration, Nucl. Phys. **A658**, 67 (1999).
[26] A. Strachan and C.O. Dorso, Phys. Rev. C **55**, 775 (1997).
[27] C. Dorso and J. Randrup, Phys. Lett. B **301**, 328 (1993).
[28] J. Bondorf *et al.*, Phys. Rep. **257**, 133 (1995).
[29] D.H.E. Gross, Rep. Prog. Phys. **53**, 605 (1990).